Molecular Crystals and Liquid Crystals Science and Technology. Section A. Molecular Crystals and Liquid Crystals
Publication details, including instructions for authors and subscription information:
http://www.tandfonline.com/loi/gmcl19

Condis Crystals of Small Molecules V. Solid State ^{13}C NMR and Thermal Properties of N,N′-b/s(4-n-Octyloxybenzal)-1,4-Phenylenediamine (OOBPD)

Jinlong Cheng [a b], Yimin Jin [a b], Guanghe Liang [a b], Bernhard Wunderlich [a b] & Hans G. Wiedemann [c]

[a] Department of Chemistry, University of Tennessee, Knoxville, TN, 37996-1600

[b] Chemistry Division, Oak Ridge National Laboratory, Oak Ridge, TN, 37831-6197

[c] Mettler Toledo Instrumente AG, CH-8606, Greifensee, ZH, Switzerland

Version of record first published: 24 Sep 2006.

To cite this article: Jinlong Cheng , Yimin Jin , Guanghe Liang , Bernhard Wunderlich & Hans G. Wiedemann (1992): Condis Crystals of Small Molecules V. Solid State ^{13}C NMR and Thermal Properties of N,N′-b/s(4-n-Octyloxybenzal)-1,4-Phenylenediamine (OOBPD), Molecular Crystals and Liquid Crystals Science and Technology. Section A. Molecular Crystals and Liquid Crystals, 213:1, 237-258

To link to this article: http://dx.doi.org/10.1080/10587259208028735

Mol. Cryst. Liq. Cryst., 1992, Vol. 213, pp. 237–258
Reprints available directly from the publisher
Photocopying permitted by license only

Printed in the United States of America

Condis Crystals of Small Molecules V. Solid State ^{13}C NMR and Thermal Properties of N,N′-*bis*(4-*n*-Octyloxybenzal)-1,4-Phenylenediamine (OOBPD)

JINLONG CHENG, YIMIN JIN, GUANGHE LIANG and BERNHARD WUNDERLICH*

Department of Chemistry, University of Tennessee, Knoxville, TN 37996-1600 and Chemistry Division, Oak Ridge National Laboratory, Oak Ridge, TN 37831-6197

and

HANS G. WIEDEMANN

Mettler Toledo Instrumente AG, CH-8606 Greifensee ZH, Switzerland

(Received August 6, 1991)

Motion in the condis and liquid crystalline phases of N,N′-*bis*(4-*n*-octyloxybenzal)-4-phenylenediamine (OOBPD) over the temperature range 187–431 K has been analyzed by solid state ^{13}C nuclear magnetic resonance under the conditions of cross-polarization transfer and magic angle spinning (CP-MAS), and ^{13}C spin-lattice relaxation times. The ^{13}C γ-*gauche* effect indicated that even in the crystals of K3 (below 385 K) conformational disorder and motion exist in the paraffin chains. Also, below the first transition temperature (K3 to K2, at 385 K), coalescence of signals suggest 180° phenylene ring flips without increase in disorder (entropy). The mobilities are evaluated using the relaxation times of ^{13}C. Heat and entropy have been determined from 130 to 550 K. From a fit of the heat capacity at low temperature to an approximate vibrational spectrum, it could be derived that a large amount of conformational entropy is introduced gradually. Corrected thermal data are given for all phase transitions. A full accounting of order and motion could be made.

Keywords: N,N′-bis(4-n-octyloxybenzal)-1,4-phenylenediamine (OOBPD), condis state, liquid crystal, conformational motion, solid state NMR, γ-gauche effect of ^{13}C, nuclear spin-lattice relaxation, DSC, heat capacity, entropy

INTRODUCTION

This series of publications[1–4] has the goal to establish the role of conformational disorder and motion in small molecules that exhibit liquid or plastic crystalline phases. In the first two papers,[1,2] it was suggested using calorimetry and structure analyses of the transitions of N,N′-*bis*(4-*n*-octyloxybenzal)-1,4-phenylenediamine (OOBPD), that the assignment of the mesophase structure K3/385.2/K2/388.2/K1/415.3/H′/422.2/G′/426.9/I/436.6/C/475.4/N/504.4/Melt (temperatures in K) could be

refined by stating that K1 to K3 are still mesophases that are conformationally disordered (condis crystals). It will be shown that it is not only possible to have a stepwise freezing of motion and disorder of the melt to nematic (N) and the various smectic phases (C, I, G′ and H′), but also to continue this stepwise freezing through several condis states (K1, K2, and K3). In addition a large amount of conformational entropy is gained outside of the transition regions. In the condis state the crystals have lost the translational disorder and mobility of the liquid crystals, but maintain still various degrees of conformational disorder and mobility.[5]

In order to fully characterize the proposed condis phases K1–K3 and their relationships to the liquid crystalline phases G′ and H′, direct observations of the mobility of both the octyloxy chains and the mesogen are made using variable-temperature solid state ^{13}C CP-MAS NMR. In addition, the heat capacity has been measured between 130 K and 550 K by DSC and fitted at low temperature to an approximate frequency spectrum. The calculated vibration-only heat capacity starts to show deviations from the measured one at about 200 K, reflecting beginning contributions of conformational disorder and motion in the octyloxy chains which is initially similar to paraffins such as octane,[6] then reaches, however, the much higher level of the liquid, so that a major entropy gain beyond that of a hypothetical rigid, vibration-only crystal occurs outside and before the sharp endothermic transition peak from K3 to K2 and K1. By combining NMR and thermal analysis evidences a full characterization of motion and disorder in OOBPD is possible.

EXPERIMENTAL

Sample

The synthesis of the OOBPD sample in our laboratory followed closely the method reported in the literature.[7] Solvent recrystallization of the OOBPD sample was performed from chloroform to increase the purity, verified by both ^{1}H and ^{13}C NMR in solution. The sample was continuously kept dry in a desiccator with anhydrous calcium chloride.

Solid State NMR

Samples were packed into the NMR rotor in a glove bag under an atmosphere of dry nitrogen gas. All the solid state ^{13}C NMR measurements were made with a Nicolet NT 200 spectrometer operating at 200.07 and 50.31 MHz for ^{1}H and ^{13}C, respectively. The solid state probe was purchased from Doty Scientific, Inc., and has a design similar to that described in the literature.[8] The probe has variable temperature capability over the range of 150–430 K. Liquid methanol and ethylene glycol were used for chemical shift thermometry to calibrate the sample temperatures below and above 300 K.[9] The cylindrical sample container (rotor) was made from a single crystal of Al_2O_3 (sapphire) and has a diameter of 5 mm. The end cap pairs used for the rotor were made from brown Vespel® (Registered trademark for a DuPont polyimide). The sample was spun with nitrogen gas at 4.5 kHz at the magic angle for all measurements. Prior to each measurement, at stabilized

temperature and with sample spinning at constant rate, the probe was tuned and matched with a 2382 Spectrum Analyzer (100 Hz–400 MHz) made by Marconi Instruments.

The variable-temperature ^{13}C spectra were measured with the technique of cross-polarization (CP) transfer and magic angle spinning (MAS). The spin contact/lock time for the CP was 1 ms and 90° pulse width for protons was 4.85 μs. During data acquisition, a high power dipolar decoupling was used (ca. 25 W, corresponding to about 50 kHz rf field strength). The ^{13}C spin-lattice relaxation time (T_1) measurements were carried out using the inversion recovery (IR) method in the observation (^{13}C) channel, while broad band two-level decoupling of the protons was maintained in the ^1H channel (with high level decoupling applied only during the periods of data acquisition). The 90° and 180° pulse widths for ^{13}C in the IR experiment were 4.06 and 8.12 μs, respectively. At each temperature 10 to 20 experimental data points (variable delays) and 64 FIDs per each data point were collected to yield T_1 values with average errors of less than 5%.

For all the spectra, the data size was 16 kilo-words (16 bits per word) for a spectral width of 6000 Hz, which results in a data acquisition time of 0.6 s. The ^{13}C chemical shift values were calibrated indirectly through a powder sample of hexamethylbenzene (17.36 ppm for the methyl carbon) to TMS (tetramethylsilane). The spectrometer field drifting during a variable temperature run was estimated to be less than 0.05 ppm.

The molecular structure identification and purity of the sample were verified by solution (in deuterated chloroform) ^1H and ^{13}C NMR spectra with a Bruker AMX 400 spectrometer, operating at 400.13 and 100.62 MHz for ^1H and ^{13}C, respectively. A solution ^{13}C spectrum was also obtained on the same Nicolet NT 200 for direct comparison with the variable temperature solid state spectra.

Calorimetry

Heats of transition and heat capacities of OOBPD were measured using the Thermal Analyst 2100 System from TA Instrument Inc. with a 912 Dual Sample DSC and a DSC Autosampler. The heating rates were 10 K/min and measurement was done under a nitrogen flow at 15 ml/min. A single-run heat capacity technique was used for the measurements which was discussed in detail in previous publications.[10–12] The OOBPD of 10–20 mg sample weight was enclosed in aluminum sample pans. The heat capacities were calibrated with sapphire, and the temperatures were calibrated at the transition temperatures of cyclohexane (T_d = 186.1 K, T_m = 279.7 K), cycloheptane (T_d = 134.8 K, T_m = 265.1 K), cyclooctane (T_d = 166.5 K, T_m = 288.0 K), 1-chlorobutane (T_m = 150.1 K), 2-chlorobutane (T_m = 141.9 K), *n*-octane (T_m = 216.4 K), naphthalene (T_m = 353.4 K), indium (T_m = 429.8 K), tin (T_m = 505.1 K), and KNO_3 (T_m = 607 K). Heat capacities were measured from 130 to 550 K with three sets of experiments (130–360 K, 330–520 K, and 510–550 K). Five repeated runs, each, were used to average for the reported data. All sample placement was done with Autosampler for increased repeatability.

Calculation of Heat Capacity

The method of heat capacity calculation for linear, solid molecules from an approximate frequency spectrum has been well documented in several publications from our laboratory, see, for example, Reference 6. In short, the heat capacity contribution of the group vibrations are computed making use of frequencies obtained from normal mode analyses of IR and Raman data of related compounds. After subtracting the group vibration contribution from the experimental heat capacity at constant volume, C_v, the remaining skeletal contribution to the heat capacity is fitted with two characteristic temperatures, Θ_1 and Θ_3, of a Tarasov function. Reversing this procedure, Θ_1, Θ_3 and the group vibrations permit the computation of the vibration heat capacity at constant volume over a wide temperature range.

Following the standard treatment, the total number of skeletal vibrational modes of OOBPD is taken to be 55, and the remaining number of group vibrational modes is 209. The detailed assignment is summarized in Table I. The group vibration frequencies as derived from our *A*dvanced *TH*ermal *A*nalysis *S*ystem (*ATHAS*) data bank are listed in Table II. A universal constant A_0 (3.0×10^{-3} K mol/J) was used to convert the experimental C_p to C_v [$C_v = C_p(1 - 3RA_0T/T_m]$.[13] Because heat capacity measurements started at 130 K, only Θ_1 could be determined to be 593 ± 1 K. A typical value for Θ_3 was guessed at to be 80 K. It will not influence the calculated C_p above about 100 K, but should improve the extrapolated low-temperature data. The average and RMS errors between the experimental data reported below and the calculated C_p are 0.13 ± 1.2% from 140 to 250 K, the temperature range for which the heat capacity is predominantly vibrational. The results of the computation from 0 to 600 K are shown in Figure 1.

RESULTS

The solution ^{13}C NMR spectrum and the variable temperature solid state ^{13}C CPMAS NMR spectra are shown in Figure 2a for the mesogenic group and Figure

TABLE I

Number of groups and vibrations in OOBPD

Group	Number of Groups in Molecule	Number of Group Vibrations	Number of Skeletal Vibrations
$-CH_3$	2	2×9 = 18	2×3 = 6
$-CH_2-$	14	2×(7×7−1)* = 96	2×7×2 = 28
$-C_6H_4-$	3	3×27 = 81	3×3 = 9
$-O-$	2	2×2* = 4	2×2 = 4
$-CH=N-$	2	2×5 = 10	2×(2+2) = 8
Total		209	55

* Note that in a C−O−C sequence there are two O−C stretching frequencies, decreasing the $-CH_2-$ sequence by one C−C stretching frequencies and adding it to the $-O-$. The skeletal vibrations would have to be separated furthermore into inter and intramolecular vibrations. The Tarasov model accomplishes this separation by assigning a proper Θ_3/Θ_1 ratio.

TABLE II

Group vibrational frequencies of OOBDP

Vibrational Mode	Frequencies (K)		N	OOBPD	OOBPD
$-CH_3$ (from PP etc.)					
CH_3 as. stretch	4262		1.00	2N	2.00
CH_3 as. stretch	4259		1.00	2N	2.00
CH_3 sym. stretch	4147		1.00	2N	2.00
CH_3 as. bend	2107		1.00	2N	2.00
CH_3 as. bend	2101		1.00	2N	2.00
CH_3 sym. bend	1987		0.25	2N	0.50
	1973	1987	0.38	2N	0.76
	1973		0.37	2N	0.74
$C-CH_3$ stretch	1568	1614	0.44	2N	0.88
	1534	1614	0.56	2N	1.12
CH_3 rock ($+CH_2$ wag)	1453	1521	0.55	2N	1.10
	1453		0.45	2N	0.90
CH_3 rock($+C-C$ chain stretch)	1361	1393	0.65	2N	1.30
	1333	1361	0.21	2N	0.42
	1336		0.14	2N	0.28
Total			9.00		18.00
$-CH_2-$ (from PE etc.)					
CH_2 as. strecth	4148		1.00	14N	14.00
CH_2 sym. stretch	4098		1.00	14N	14.00
CH_2 bend	2075		1.00	14N	14.00
CH_2 wag	1698	1977	0.65	14N	9.10
	1977		0.35	14N	4.90
CH_2 twist & rock	1690	1874	0.48	14N	6.72
	1874	1874	0.52	14N	7.28
$C-C$ stretch	1378	1638	0.34	12N	4.08
	1378	1525	0.35	12N	4.20
	1525		0.31	12N	3.72
CH_2 rock & twist	1494		0.04	14N	0.56
	1038	1494	0.59	14N	8.26
	1079		0.37	14N	5.18
Total			7.00		96.00
$-C_6H_4-$ (from PPP etc.)					
CH stretch	4400		4.00	3N	12.00
$C-C$ stretch	2352	2389	1.00	3N	3.00
$C-C$ stretch	2369	2379	0.30	3N	0.90
	2284	2369	0.70	3N	2.10
$C-C$ stretch CCH bend	2172		0.26	3N	0.78
	2172	2251	0.55	3N	1.65
	2251		0.19	3N	0.57
$C-C$ stretch CCH bend	2071		0.44	3N	1.32
	2071	2136	0.56	3N	1.68

TABLE II (*continued*)

Vibrational Mode	Frequencies (K)		N	OOBPD	OOBPD
$-C_6H_4-$ (from PPP etc.)					
CCH bend	1910		0.29	3N	0.87
	1910	1966	0.50	3N	1.50
	1966		0.21	3N	0.63
C–C stretch	1838	1854	1.00	3N	3.00
C–C stretch	1824	1858	1.00	3N	3.00
C–C stretch, CCH bend	1621		1.00	3N	3.00
C–C stretch, CCH bend	1546		1.00	3N	3.00
C–C str, CCC bend, CCH bend	1480	1512	1.00	3N	3.00
C–C str, CCC bend, CCH bend	1392		0.22	3N	0.66
	1392	1464	0.55	3N	1.65
	1464		0.23	3N	0.69
C–C stretch, CCC bend	1162	1217	0.33	3N	0.99
	932	1162	0.56	3N	1.68
	926	932	0.11	3N	0.33
CCC bend, CCH bend	866	892	1.00	3N	3.00
C–C str. CCC bend	636	662	0.30	3N	0.90
	439	636	0.59	3N	1.77
	433	439	0.11	3N	0.33
CH wag	1382		1.00	3N	3.00
CH wag	1359		1.00	3N	3.00
CH wag	1200		1.00	3N	3.00
CH wag	1136	1207	1.00	3N	3.00
C–C deform, C–C torsion	1016	1093	1.00	3N	3.00
C–C deform, C–C torsion	659	770	0.56	3N	1.68
	770	806	0.44	3N	1.32
C–C torsion	577		1.00	3N	3.00
Additional	60	90	2.00	3N	6.00
Total			27.00		81.00
–O– (from POP, PO, etc.)					
C–O stretch	1385		0.11	2N	0.22
	1632		0.06	2N	0.11
	1385	1632	0.34	2N	0.67
O–C stretch	1305		0.50	2N	1.00
O–Ar stretch	1800		1.00	2N	2.00
Total			2.00		4.00
–CH=N–					
CH stretch	4347		1.00	2N	2.00
CH bend	1016	1914	2.00	2N	4.00
C–N stretch	1502		1.00	2N	2.00
C=N stretch	2302		1.00	2N	2.00
Total			5.00		10.00

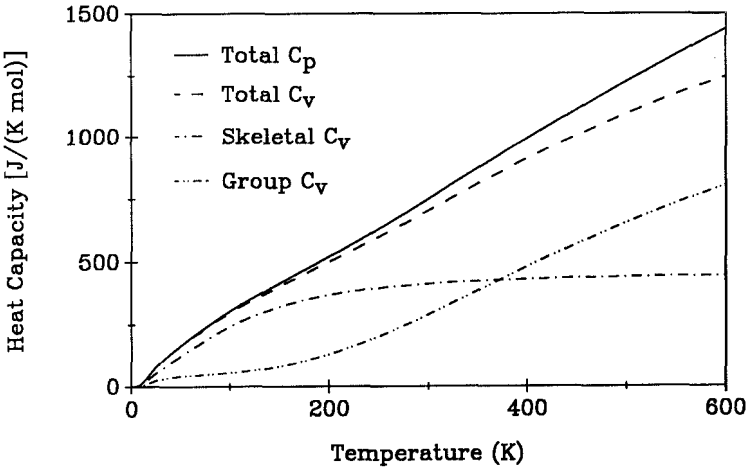

FIGURE 1 Calculated C_p of OOBPD.

2b for the octyloxy chains. The chemical shift assignments are made based on the considerations given in the Discussion, and results are shown in Table IIIA and IIIB for mesogen and octyloxy carbons, respectively. The ^{13}C T_1 data at selected temperatures are presented in Table IV.

Table V gives a list of the averages of the measured C_p as well as calculated C_p and Table VI summarizes the newly measured transition parameters making use of the improved baseline set by the vibrational heat capacity of Fig. 1 and detailed in the Discussion. The heat capacity in the liquid state, $C_{p,liq}$, could, as usual, be fitted to a linear equation:

$$C_{p,liq} = 1433.2 - 0.3084T \quad (1)$$

where T is temperature in kelvin and C_p is the heat capacity in J/(K mol). The average and RMS errors between experimental and fitted C_p is $-0.001 \pm 0.04\%$ (530 to 550 K).

DISCUSSION AND INTERPRETATION

Chemical Shift Assignments of the Solution NMR Spectrum

A correct assignment of chemical shifts (δ values) to the individual carbon atoms is important because the δ value is sensitive to the molecular motion *and* conformation. The molecular structure is represented in the following, with the three phenylene rings of the mesogen being drawn coplanar (the most stable confor-

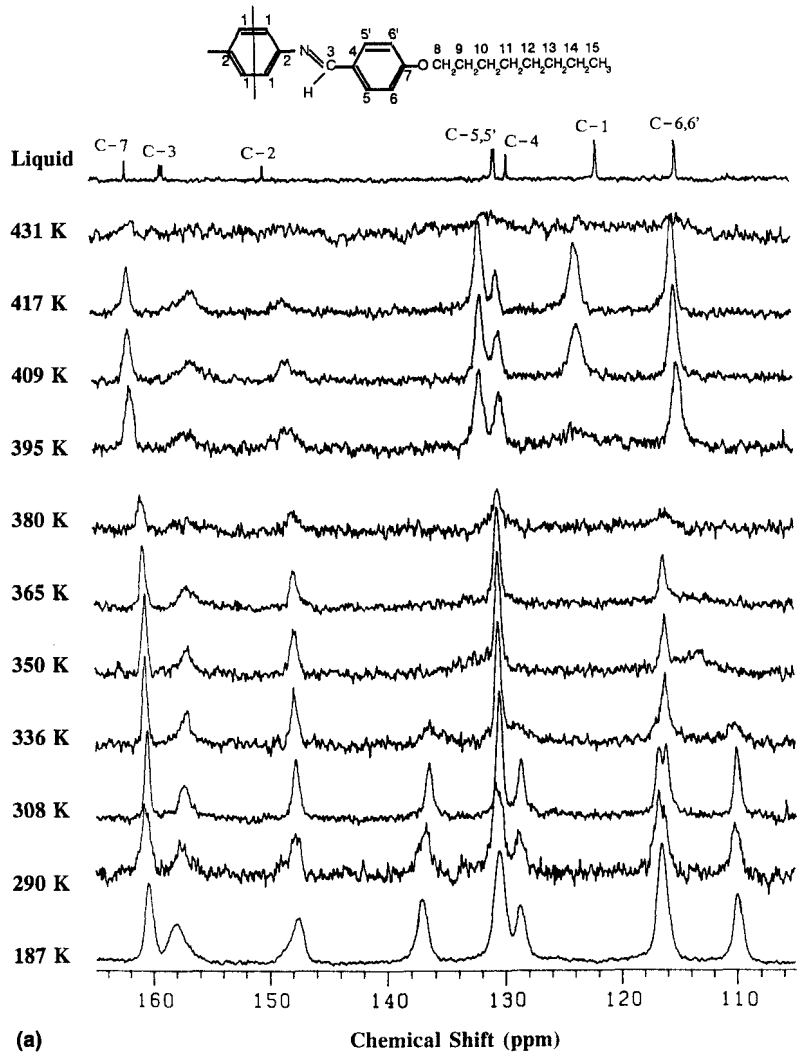

FIGURE 2 Variable temperature solid state ^{13}C CPMAS and solution ^{13}C NMR spectra of OOBPD. 2A. Spectra for mesogenic group plotted from 105 to 170 ppm, 2B. Spectra for octyloxy chain plotted from 10 to 70 ppm. Temperatures for the solid state NMR measurements are: from bottom to top, 187, 290, 308, 336, 350, 365, 380, 395, 409, 417 and 431 K. Solution spectrum is plotted at the top. Chemical shifts and T_1 data are given in Tables III and IV, respectively.

mation). The distinguishable carbon atoms in the mesogen unit are numbered. The carbons in the paraffinic groups are numbered in sequence from C-8 (for OCH_2) to C-15 (for the CH_3).

The measurement of an NMR spectrum in the melt was not possible because the melting temperature for OOBPD (505.4 K) is higher than the highest allowable temperature of the NMR probe (430 K). The melt spectrum is, nevertheless, expected to be the same as a solution spectrum because the molecular motion should be similar in both liquids. Therefore, the solution spectrum has been com-

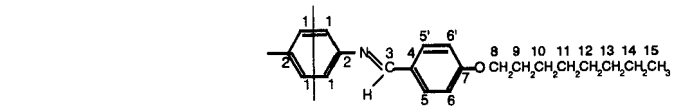

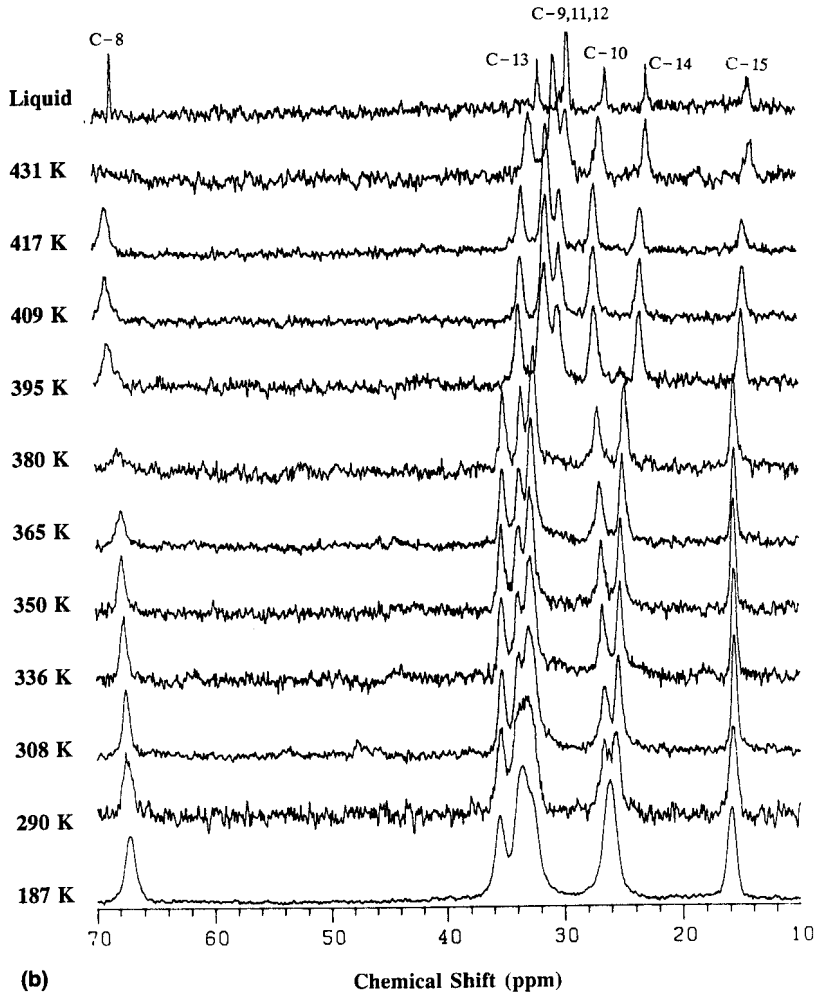

FIGURE 2 (*continued*)

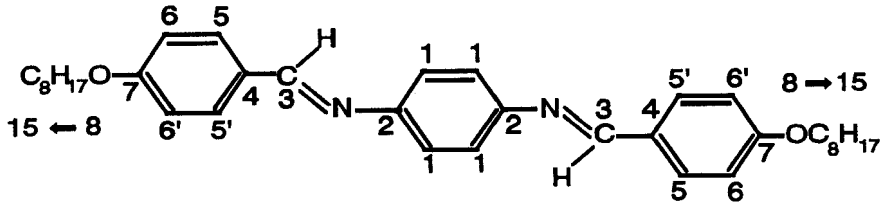

TABLE III

^{13}C NMR chemical shifts (ppm)[a] for OOBPD at selected temperatures and in solution[b]

	A Mesogenic Group								
	C-1[c]	C-2	C-3	C-4	C-5	C-5'	C-6	C-6'	C-7
187 K	116.4	147.5	158.0	130.4	128.7	137.0	109.9	116.4	160.4
290 K	116.7	147.8	157.5	130.7	128.9	136.7	110.2	116.7	160.7
308 K	116.1	147.7	157.3	130.4	128.6	136.5	110.0	116.7	160.4
336 K	116.1	147.8	156.9	130.5	129.1	136.4	110.3	116.1	160.6
350 K	116.2	147.7	156.9	130.5	NO[d]	NO	113.1	NO	160.6
365 K	116.2	147.8	156.9	130.5	NO	NO	NO	NO	160.7
380 K	116.0	147.9	156.8	130.4	NO	NO	NO	NO	160.9
↕	Transitions from phase K3 to K2 (385.2 K), to K1 (388.2 K)[e]								
395 K	124.1	148.5	156.5	130.3	131.9	131.9	114.9	114.9	161.8
409 K	123.5	148.4	156.4	130.2	131.8	131.8	115.1	115.1	161.8
↕	Transition to Phase H' (415.3 K)								
417 K	123.6	148.5	156.3	130.3	131.8	131.8	115.2	115.2	161.8
↕	Transitions to Phase G' (422.2 K), to I (426.9 K)								
431 K	NO	NO	NO	NO	NO	NO	NO	NO	NO
↕	Transitions to Phase C (436.6 K), to N (475.4 K), to Melt (505.4 K)								
Solut.	121.7	150.1	158.7	129.4	130.5	130.5	114.8	114.8	161.9

	B Octyloxy Chain							
	C-8	C-9	C-10	C-11	C-12	C-13	C-14	C-15
187 K	67.11	35.45	26.06	33.49	32.82	33.85	26.06	15.80
290 K	67.45	35.31	26.58	33.40	33.40	33.85	25.55	15.77
308 K	67.39	35.30	26.62	33.02	33.02	33.84	25.41	15.77
336 K	67.50	35.31	26.74	32.83	32.83	33.85	25.22	15.64
350 K	67.65	35.25	26.76	32.83	32.83	33.76	25.11	15.64
365 K	67.76	35.20	26.95	32.71	32.71	33.80	24.98	15.62
380 K	68.00	35.07	27.04	32.45	32.45	33.51	24.71	15.57
↕	Transitions from phase K3 to K2 (385.2 K), to K1 (388.2 K)							
395 K	68.86	31.44	27.29	30.34	31.44	33.72	23.46	14.87
409 K	68.94	31.25	27.21	30.16	31.25	33.45	23.35	14.70
↕	Transition to Phase H' (415.3 K)							
417 K	68.89	31.38	27.12	30.34	31.13	33.31	23.27	14.65
↕	Transitions to Phase G' (422.2 K), to I (426.9 K)							
431 K	NO	30.51	26.69	29.49	30.51	32.66	22.72	13.95
↕	Transitions to Phase C (436.6 K), to N (475.4 K), to Melt (505.4 K)							
Solut.	68.35	29.29	26.10	29.29	29.29	31.84	22.67	14.00

a. Spectra are shown in Fig. 2 and the chemical shift values are relative to tetramethylsilane (TMS).
b. In d-$CHCl_3$ solution at room temperature.
c. Numbering and assignment of the carbon atoms is given in the text.
d. "NO" stands for no signal is observable.
e. The transition parameters are taken from Wiedemann.[2]

TABLE IV

^{13}C NMR spin-lattice relaxation times (s)[a] for OOBPD at selected temperatures

	Mesogenic Group								
	C-1[b]	C-2	C-3	C-4	C-5	C-5'	C-6	C-6'	C-7
308 K	>100[c]	>100	>100	>100	>100	>100	>100	>100	>100
350 K	>100	>100	>100	>100	>100	>100	>100	>100	>100
380 K	157.8	282.0	7.81	123.6	NO[d]	NO	NO	NO	40.00
↕	Transitions from phase k3 to K2 (385.2 K), to K1 (388.2 K)[e]								
395 K	5.19	15.5	1.25	8.20	0.96	0.96	0.81	0.81	11.4
↕	Transition to Phase H' (415.3 K)								
417 K	0.72	16.0	0.70	5.14	0.25	0.25	0.24	0.24	8.26
↕	Transitions to Phase G' (422.2 K), to I (426.9 K), to Phase C (436.6 K), to N (475.4 K), to Melt (505.4 K)								

	Octyloxy Chain							
	C-8	C-9	C-10	C-11	C-12	C-13	C-14	C-15
308 K	>100	>100	>100	>100	>100	>100	>100	Not Ava.
350 K	>100	17.0	12.6	15.5	15.5	19.5	12.6	4.70
380 K	37.9	12.9	6.58	13.2	13.2	9.76	12.2	8.52
↕	Transitions from phase K3 to K2 (385.2 K), to K1 (388.2 K)							
395 K	2.59	1.77	1.35	2.04	1.77	3.72	4.09	7.27
↕	Transition to Phase H' (415.3 K)							
417 K	1.29	1.58	1.24	1.93	1.58	3.16	4.10	8.06
↕	Transitions to Phase G' (422.2 K), to I (426.9 K), to Phase C (436.6 K), to N (475.4 K), to Melt (505.4 K)							

a. Measured with Inversion Recovery method.
b. Numbering and assignment of the carbon atoms is given in the text.
c. T_1 is longer than 100 s.
d. "NO" stands for no signal is observable, therefore, the T_1's are not available.
e. The transition parameters are taken from Wiedemann.[2]

pared with the spectra of the solid state at lower temperatures. With the solution spectrum shown in Figure 2A and 2B, one can make the δ assignments for all the carbons as shown in Table IIIA and IIIB.

The assignment of the methylene ^{13}C's in the octyloxy chain (see Table IIIB) was made by comparing with the spectrum of *n*-octane whose ^{13}C δ values are known to be, from the end (methyl) to the center, 14.2, 23.2, 32.6, and 29.9 ppm.[14] In OOBPD the chemical shifts of methylene carbons of the octyloxy chain are, however, subject to the influence of *substituent effects* of the oxygen. The available data[15] on the alkyl carbons of aralkyl ethers (with the group of phenylene-oxygen-

TABLE V

Measured and calculated heat capacities of OOBPD

Temperature (K)	Measured C_p [J/(K mol)]	Calculated C_p[a] [J/(K mol)]	Deviation[b] (%)
130.00	390.53	373.78	-4.29
140.00	401.18	395.50	-1.41
150.00	415.67	416.67	0.24
160.00	430.88	437.34	1.50
170.00	451.11	458.03	1.53
180.00	471.07	478.81	1.64
190.00	494.44	499.57	1.04
200.00	516.15	520.68	0.88
210.00	540.16	541.79	0.30
220.00	564.95	563.37	-0.28
230.00	590.12	585.61	-0.76
240.00	615.72	607.81	-1.28
250.00	642.69	630.73	-1.86
260.00	671.82	653.41	-2.74
270.00	701.81	676.92	-3.55
273.15	713.23	684.31	-4.06
280.00	739.82	700.51	-5.31
290.00	775.93	724.67	-6.61
298.15	805.69	744.42	-7.60
300.00	812.66	748.93	-7.84
310.00	851.89	773.36	-9.22
320.00	894.07	797.80	-10.77
330.00	939.64	822.39	-12.48
340.00	989.06	846.76	-14.39
350.00	1043.52	871.64	-16.47
360.00	1108.43	896.28	-19.14
370.00	1194.15	920.97	-22.88
380.00	1310.56	945.78	-27.83
↕	Transitions from phase K3 to K1, to H', to G', to I, to C, to N, to Melt		
530.00	1270.12	1269.78	-0.03
540.00	1266.06	1266.69	0.05
550.00	1263.95	1263.61	-0.03

a. Before transitions, data are calculated from approximate frequency spectra for solid. After transition, data are calculated from Eq. (1).

b. Deviation (%) = 100 (1 - $C_{p,expt}$ / $C_{p,calc}$)

alkyl) show that when the alkyl chain consists of more than 5 carbons, the oxygen has positive substituent effects (deshielding) of +55 and +5.8 ppm on the α- and β-carbons, i.e. C-8 and C-9, respectively. Thus, the measured values of 68.35 and 29.29 ppm are assigned to C-8 and C-9, respectively. The oxygen, however, has a negative substituent effect (shielding) of about −6.5 ppm on the γ-carbon, which causes C-10 to resonate at 26.10 ppm. The rest of the carbons are not influenced by the oxygen. Their δ values agree well with the respective carbons in *n*-octane. The signals of C-11 and C-12 are one single, intense peak at 29.29 ppm, overlapping

TABLE VI

Transition parameters of OOBPD

Transition	T (K)		ΔH (kJ/mol)		ΔS [J/(K mol)]	
	S-C[a]	M-C[a]	S-C	M-C	S-C	M-C
K3-K1	386.51	385.50	18.45	18.12	47.73	46.99
K1-H'	415.66	415.35	9.60	9.54	23.10	22.96
H'-G'	421.74	421.80	2.53	2.55	6.00	6.05
G'-I	427.15	427.18	0.55	0.58	1.28	1.37
I-C	436.85	436.73	3.93	3.79	9.00	8.69
C-N	476.66	476.46	5.24	5.28	10.99	11.09
N-Melt	504.85	504.76	4.12	4.49	8.17	8.90
Total			44.42	44.36	106.27	106.04

a. S-C: solution-crystallized; M-C: melt-crystallized.

with C-9, while C-13, C-14 and C-15 appear at 31.84, 22.67 and 14.00 ppm, respectively.

For the aromatic carbons, the assignments can also be made based on the consideration of substituent effects. Detailed values of the substituent effects on aromatic ^{13}C's can be found in the literatures.[14,16] The predicted values are in good agreement with the measured ones. Table IIIA summarizes the results for all carbon atoms in the mesogenic group.

Conformational Isomers

Generally, the appearance of the solid state ^{13}C NMR spectra changes with temperature, indicating the change of molecular conformation and mobility. The effects of intermolecular packing are usually small. For OOBPD one looks for two possible types of motion. One, which may be present in the mesogenic group and the other, in the methylene groups. The motion is expected to involve phenylene ring flips and rotations about C—C bonds to populate other rotational isomers, respectively. The two segments of the molecule will be discussed separately.

Mesogen. Figure 2A shows that, except at 431 K (where the carbons in the mesogenic group show hardly any resonances), all solid state ^{13}C spectra at and above 395 K are similar to the solution spectrum, therefore, the δ values of Table IIIA are close to that of the solution.

In the spectrum at 380 K, below the transition to the K3-phase, the δ's of all nonprotonated carbons, C-2, C-4, and C-7 as well as the methine carbon C-3 remain still approximately the same and continue at these values down to the lowest temperature measured (187 K), while the δ for the protonated aromatic carbons, namely C-1, C-5, C-5′, C-6, and C-6′ change significantly. The δ value for C-1 changes from 124.1 ppm at 395 K to 116.2 ppm at 365 K. The signals for C-5, C-5′ become not observable at 380 and 365 K, and split into a pair as the temperature decreases further from 350 to 308 K. The same is also observed for C-6

and C-6′. At 321 K (the spectrum is not shown, but is very similar to that of 308 K) and below, signals of C-5 and C-5′ can be observed at about 136.5 and 128.6 ppm, respectively. While C-6 and C-6′ resonate at about 116.7 (distinguishable from C-1 at 116.1 ppm), and 110.0 ppm, respectively.

These features of the mesogen indicate the process of an increasing mobility of 180° phenylene ring flipping with increasing temperature. At temperatures below 321 K, the absence of the ring flip induces inequivalence in two pairs of carbon atoms on the ring, namely C-5/C-5′ and C-6/C-6′. The C-5 is more shielded (smaller δ value) than C-5′ because of the stronger steric interaction arising from the shorter distance between C-5 and H-3 (the proton attached to C-3). The same argument holds also for C-6 and C-6′. As temperature is increased to about 336 K, the phenylene rings become mobile. If the motion is that of a rotation about its 1,4 axis (flipping), C-5 will exchange position with C-5′, and C-6 with C-6′. When the rate of the flipping is comparable to the frequency separation of the signals at lower temperatures (about 400 Hz for C-5/C-5′, and 325 Hz for C-6/C-6′), coalescence of the signals is to be observed. The spectra at 336 and 350 K show the onset of this coalescence, where the spectral lines are too broad to be observed. At temperatures higher than the transition to the K1 state (385 K), the sufficiently fast phenylene ring flipping averages between C-5 and C-5′ as well as C-6 and C-6′, resulting in average positions of 131.9 and 114.9 ppm for C-5/C-5′ and C-6/C-6′, respectively.

The coalescence of the signals of a pair of carbon atoms that are inequivalent in the solid state has been observed for a residue of bisphenol A by Garroway and co-workers.[17–19] The signals of two *meta*-carbons (meta to the oxygen) were observed to be distinct over the temperature range 150–350 K, and then undergo coalescence at higher temperatures as motional averaging occurs. The same situation was also found for the two *ortho*-carbons in the bisphenol A residue. The inequivalency of the ^{13}C's is the identical symmetry positions in the phenylene rings of poly(*p*-hydroxybenzoic acid) and poly(2,6-dimethoxy *p*-hydroxybenzoic acid) was also observed in the solid state.[20]

The phenylene ring flipping starting gradually at about 336 K in OOBPD occurs considerably lower than the first sharp transition. This temperature and the observed entropy change of 47 J/(K mol) will be shown below to be largely the consequence of disordering in the paraffin chains. The total combined entropy of all transitions at higher temperatures, i.e., at H′, G′, I, C, N, and melting, is about 59 J/(K mol) from the present measurement, somewhat larger than the earlier value of 41.6 J/(K mol) of Wiedemann *et al.*,[2] because of a better baseline adjustment. This value is close to the typical value of 20 to 59 J/(K mol) for the positional and orientational disordering of a single, rigid, nonspherical motif (average value 36 ± 10 J/(K mol), anthracene = 58.9 J/(K mol)).[21]

In OOBPD, the motionally averaged δ value of 131.9 ppm for C-5/C-5′ at higher temperatures is approximately the middle of the two resonances at lower temperature, 132.6 ppm, while the δ value for C-6/C-6′ at higher temperatures, 114.9 ppm, differs somewhat from the middle of the two at lower temperature, 113.4 ppm. All C-1 carbons appear to be equivalent at any temperature by having a single peak. This is probably due to the rather long distance between the central

phenylene ring and H-3 that renders C-5 and C-6 to be inequivalent from C-5′ and C-6′, respectively, at low temperatures. The temperature at which the δ of C-1 changes is well within the ranges of the transitions between the K phases (385–388 K), the signal jumps from 116 ppm at 380 K to about 124.1 ppm at 395 K.

The rate constant, k, of the ring flip at coalescence temperatures, 336–380 K, can be evaluated from exchange-broadened NMR spectra, using one of the most widely used expressions[22]:

$$k = \pi(\delta\nu)/\sqrt{2} \tag{2}$$

where $\delta\nu$ is the frequency separation of the signals below the temperatures of coalescence. As shown above, $\delta\nu$ is about 400 Hz at 308 K, thus at the coalescence temperatures centered at 365 K, the rate of the ring flipping is about 900 s^{-1}.

The ^{13}C spin-lattice relaxation time, T_1, as given in Table IV, can be used to evaluate the mobility and to support the δ assignments made above. In the solid state the motional correlation time is usually on the long-time side of the T_1 minimum (except for the methyl carbon). Therefore, as the mobility increases because of the temperature increase, the values of T_1 are expected to decrease. This prediction is generally fulfilled as shown in Table IV.

At 350 K and below, the T_1's of the ^{13}C's in the mesogenic group are estimated to be much longer than 100 s, indicating the fact that the motion in this part of the molecule is frozen. As the temperature is increased from 380 to 395 K, to pass the transitions to K2 and K1, T_1 for the observable carbons, C-1, C-2, C-3, C-4, and C-7, decreases drastically by a factor of 10 or more. At the temperature just above the K transitions, 395 K, the C-1 of the central ring shows a much longer T_1 (5.19 s) than either C-5/C-5′ (T_1 0.96 s) or C-6/C-6′ (T_1 0.81 s) in the side rings. This is also true at the even higher temperature of 417 K, although the difference is less profound. This indicates clearly that the motion in the central ring is slower than the side rings at a given temperature.

It is interesting to examine the relaxation behavior of C-4. Its T_1 is much shorter than that of C-2 and C-7. This is most likely due to the proximity between C-4 and H-3, which provides an effective relaxation mechanism through the dipolar interaction between them. Thus H-3 serves to: (1) provide a relaxation pathway for C-4, (2) render the inequivalence between C-5 and C-5′ as well as between C-6 and C-6′ at low temperatures, (3) impose an energy barrier to the rotation of the side rings via the steric interaction with H-5 or H-5′.

n-Octyloxy groups. The appearance of the ^{13}C NMR spectrum in this part of the molecule has a rather different temperature dependence from that of the mesogen. For convenience of analysis, the carbons are grouped into two types according to the variation of their δ values. As shown in Figure 2B and Table IIIB, type I carbons are those carbons that have almost constant δ values over the entire range of experimental temperature. This type of ^{13}C can be easily recognized as C-8, C-10 and C-15, whose resonances at 308 K are at 67.39, 26.62 and 15.77 ppm, respectively. The C-13 resonates at 33.84 ppm at 308 K may also be attributed to the type I for reasons that will be given below. The rest of the carbons whose δ values decrease with temperature (up-field shifting) belong to type II.

In the solid state, even though the molecules are packed in close proximity and their δ reflects these packing effects, one finds that the intramolecular conformations are the most important influence on δ. Specifically, the δ's are influenced by the substituents attached to the observed carbon at the α-, β- and γ-positions, called α-, β- and γ-substituent effects. The first two effects have fixed contributions to the δ value of the observed carbon as long as the chemical structure of the molecule is fixed. The γ-substituent effect, however, has a conformational origin,[23,24] because the observed carbon, °C, and its γ-substituent, ᵞC, are separated by three intervening bonds, $^{\circ}CH_2$—CH_2—CH_2—$^{\gamma}CH_2$, and their mutual distance and orientation are variable, depending on the conformation of the central bond (or rotational isomeric state). For a ^{13}C to be more shielded by a γ-substituent, the °C and ᵞC must be in a *gauche* arrangement, and the effect of γ-*gauche* shielding can be evaluated to be $\gamma_{C-C} = -5.2$ ppm.[25] In the melt or solution, the rotating C—C bonds are expected to have a population of 40% *gauche* conformation, a value adopted by Flory for melt of polyethylene,[26] one would expect, after a transition from fully ordered all-*trans* to 40% of *gauche*, the δ of the ^{13}C to decrease (be more shielded) by:

$$\Delta\delta = 2 \times (0.4) \times (-5.2) \text{ ppm} = -4.16 \text{ ppm}$$

The factor of two accounts for the two possible γ-substituents at both sides of the observed carbon. If only one of the two γ-substituents has become *gauche* to °C, the Δδ would be −2.08 ppm. Similarly, if neither of the γ-substituents has changed its spatial relationship with °C, the Δδ is zero. Overall, as temperature is increased, the δ of a ^{13}C in the linear paraffinic chains may change by an amount of almost 0, −2, or −4 ppm. For OOBPD, the type I carbons are thus expected to have Δδ of close to 0, and type II close to either −2.08 or −4.16 ppm, depending on the number of ᵞC's that become *gauche* to the °C.

For type I carbons C-8, C-10, and C-15 (and also C-13 as will be shown next), the chemical shifts in Figure 2B and Table IIIB remain constant over temperature range 187–431 K, and are also very close to that of the liquid. This comparison immediately implies that C-8, C-10, and C-15 already possess *gauche* character comparable to the value in the solution. The corresponding bonds are marked with the sign ¤ in Figure 3.

The methyl rotation is also marked in the diagram, because its motion is known to start at the lowest temperature of any other conformational motion.[27] Based on Figure 3 as developed to this point, one can easily predict δ for C-13. The δ of C-13 is expected not to change with temperature because the only bond that may cause the C-13 signal to move up-field is already known to be of some *gauche* content at very low temperature from the behavior of C-10 (between C-11 and C-12). Thus, the signal of 33.84 at 308 K must, with certainty, be assigned to C-13, permitting the full correlation of liquid and solid spectra.

It should be noted that about the bonds marked ¤ in Figure 3, the *trans* conformation is still possible with a chance of perhaps 60%, and because of rotational motion the conformations must change with time. The actual conformation of a given bond depends on the conformation of the nearest-neighbors, as well as the

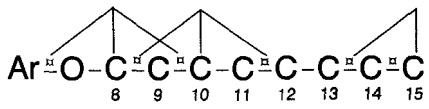

FIGURE 3 Bond conformations of the octyloxy chain below the K transitions. The bonds marked with the sign ¤ are of the *gauche* character indicated by the constant chemical shifts of C-8, C-10 and C-15, accordingly.

mode of intermolecular packing. Nearest neighbors may not have simultaneously *gauche* conformations (pentane effect[26,28]) and in order to maintain largely parallel packing, only kinks or jogs as detailed by Pechhold[21,29] can be placed along the octyloxy chain. With three of the bonds fixed in the *trans* conformation it is possible to have 2g1, 2g2, 2g3, or 3g2 kinks. Due to the equilibrium concentration of *gauche* in the liquid being about 40% and the specific geometry of the kinks larger than 2g2, one expects at an average only one of these defects at any one time in each of the octyloxy chains.

From the analysis of γ-*gauche* effect on group I carbons, one derives thus that the octyloxy chains have already developed considerable conformational freedom at temperatures below *any* transitions observed in this and the earlier calorimetric work.[2] These bonds, therefore, cannot have contributed to the earlier observed total entropy change over the various stages of fusion of 87.2 J/(K mol). Similar conformationally disordered crystals were also demonstrated by the thermal properties of some segmentally fluorinated paraffins and one- or two-dimensionally rigid mesogens substituted with flexible alkane chains.[30] Easily recognizable phases with mobile alkanes (condis crystal phases) can be identified in these cases.

One consequence of the decrease in the mobility at low temperatures should be an increase in the linewidth. The linewidth of the spectrum at 187 K shown in Figure 3B is 50 Hz, while that of 310 K is only 20 Hz. The line broadening may be due to two possible causes: (1) A motion in the 10^4-10^5 Hz region has become dominant. This motion is too slow to completely average the dipolar interactions (the major factor of line broadening in the solid state), and the effect of dipolar broadening can neither be removed by realistically achievable proton decoupling fields, nor with the magic angle spinning speeds.[31,32] It was shown[33] that under high power decoupling the average Hamiltonian of the interchain heteronuclear dipolar interactions increases gradually while the rate of the motion approaches the frequency-equivalent of the decoupling field strength, therefore, the linewidth increases. (2) The conformational motion may have been frozen. In this case the broadening arises from the dispersions of isotropic chemical shifts (distribution of frozen conformations). Such dispersions are common in the glassy state.[30,31] The spectrum of a semicrystalline polyethylene[34] shows the line width of 15 Hz for the crystalline resonance, while that of the noncrystalline resonance (appears at upfield by 2.3 ppm) is ca. 40–50 Hz.

At this point, it is not known whether in OOBPD shift-dispersion or incomplete motional narrowing, or both account for the increased line width at 187 K. It would be, however, of interest to follow the spectrum to even lower temperature at which all the motion is quenched. One expects to see additional changes in the δ values particularly for the type I carbons. At such low temperature the all-*trans* crystalline

carbons show sharp resonances at lower field, while an amorphous glass would feature broadened lines.

To resolve this problem under the given constraints of temperature, i.e., to find out at what temperature the motion in the bonds marked ¤ in Figure 3 starts, the heat capacity for the vibration-only case (Figure 1) has been calculated to compare with the measured one. The results, discussed below, show that the motion starts at about 200 K, just at the lowest experimental temperature of our NMR probe (approximately 190 K).

For the type II carbons C-9, C-11, C-12 and C-14, abrupt changes in their δ values can be seen at the transition to the K1 state. The δ of C-14 decreases by $\Delta\delta = -1.25$ ppm, C-11 by -2.11 ppm, C-12 by -1.01 ppm, and C-9 by -3.63 ppm. The large change in δ of C-9 is due to two γ-*gauche* effects (the bonds O—C8 and C10—C11). The overall change is that of "fusion" of about two or three *trans* bonds (marked with ¤ in Figure 3), or four to six for the total molecule. From these 4–6 bonds one expects an entropy change of $(4-6) \times 9.5$ J/(K mol) = 38–57 J/(K mol) for the transitions, which matches the observed value of 47 J/(K mol) (Table VI).

At temperatures above the K transitions, small decreases in the δ values can still be observed for all the carbons, especially for C-9 and C-12 that overlap at 31.44 ppm at 395 K. These decreases in δ values are much less than that observed at the transitions to the K1 phase, and can be easily attributed to the expected gradual increase in the *gauche* conformation with temperature.

Spin-lattic Relaxation Times

While the γ-*gauche* effect has been used to predict the overall changes in bond conformations, the nuclear spin relaxation times, shown in Table IV, are useful to reveal their mobilities. Except for the methyl carbon (C-15), the T_1 of all other ^{13}C at temperatures below 350 K is estimated to be much longer than 100 s, indicating slow motion and causing the convensional one-pulse with two-level decoupling (BILEV) pulse sequence fail to detect any signal. As the temperature is increased to 350 and 380 K, which is still in the K3 phase, the T_1's of C-9 through C-14 decrease to about 15 s, indicating that substantial motion has already started. The shorter T_1's of the octyloxy chain carbons when compared to the carbons of the mesogen indicate that the alkyl chain is more mobile than the mesogen, although ring flipping has also started. Between 350 and 380 K, a larger decrease in T_1 can be found for the type I methylene carbons C-8, C-13, and C-10 than for the group II methylene carbons. As the temperature is further increased to 395 K, just above the transition to phase K1, the T_1's of all carbons undergo a decrease. The condis phase K1 is thus much more mobile than condis phase K3. Upon going to the liquid crystalline phase H′ at 417 K, the T_1's do not change much except for C-1, C-5, and C-6. The latter is perhaps an indication that the mesogen has now lost its positional and some of its orientational order, as expected for a condis-crystal to liquid-crystal transition.

The correlation time, τ_C, of the motion in the octyloxy chain can be evaluated using the commonly assumed expression for spin-lattice relaxation by dipole-dipole interaction:

$$\frac{1}{nT_{1C}} = \frac{\gamma_C^2\gamma_H^2h^2}{40\pi^2r^6}\left[\frac{\tau_C}{1 + (\omega_H - \omega_C)\tau_C^2} + \frac{3\tau_C}{1 + \omega_C^2\tau_C^2} + \frac{6\tau_C}{1 + (\omega_H - \omega_C)^2\tau_C^2}\right] \quad (3)$$

where n is the number of directly bonded protons, h is Planck's constant, γ_C and γ_H are the carbon and proton magnetogyric ratios, respectively, r is the distance between interacting ^{13}C and ^{1}H, ω_C and ω_H are the ^{13}C and ^{1}H resonance frequencies. Using the T_1 data in Table IV, the correlation times, τ_C, on the long-time side of the T_1 minimum, defined by this equation are thus: longer than 10 μs below 350 K, decrease to 1 μs at 350 and 380 K (in the K3 phase), while in the K1 phase the correlation times decrease further to about 0.1 μs and then remain approximately the same up to the highest NMR experimental temperature in this work (417 K).

Unlike the methylene carbons, the T_1 of the methyl carbon increases within the K3 phase with temperature. Since its motion (the composite of the methyl rotation and rotations about various bonds along the chain) is fast, its correlation time is at the short-time side of the T_1 minimum. This conclusion is also in agreement with the conformational motion about the C—C bonds between C-13 and C-14 below any observed transition.

Heat Capacities and Heats of Transition

The heat capacity computed for an OOBPD crystal which shows only vibrations (Figure 1) and the heat capacity of the liquid are compared in Figures 4 and 5 with the actual measurements. One can clearly see that there are no low temperature transitions in the K3 phase as speculated about earlier to account for the low total heats of transition. A major increase in heat capacity beyond the vibration-only limit can be seen, however, beginning at about 200 K. In fact, at the beginning of the transition to the K2 and K1 phases the heat capacity has reached the level of the liquid. The entropy contributed by the shaded area of the graphs is 74.7 J/(K mol), more than the transitions from K3 to the liquid crystal H′. A more detailed discussion will be made now treating, as before, mesogen and octyloxy groups separately.

Mesogen. An increasing mobility of 180° phenylene ring flipping with temperature starting at 336 K, as shown by NMR, will not contribute much to the entropy. Since after a flip has occurred, the molecule is indistinguishable from the starting conformation. Consequently one expects also no major increase in the heat capacity due to the mesogen motion in the phase K3 (and K2 and K1). It is a well-known fact that a vibrator changing to a rotator or undergoing jump-like motion shows a gradual decrease in heat capacity over a large temperature range rather than increase, since the limiting heat capacities of vibrators and rotators are R and $R/2$, respectively.[35]

As the condis crystal K1 changes to the smectic liquid crystal, and ultimately to the melt, the jump-like motion changes to rotation and the whole mesogen undergoes orientational and positional diffusion. Indeed, all transitions from phase K1 to the melt show a combined ΔS of 59 J/(K mol), an amount close to what is expected for such motion and the resulting disorder, as was outlined above.

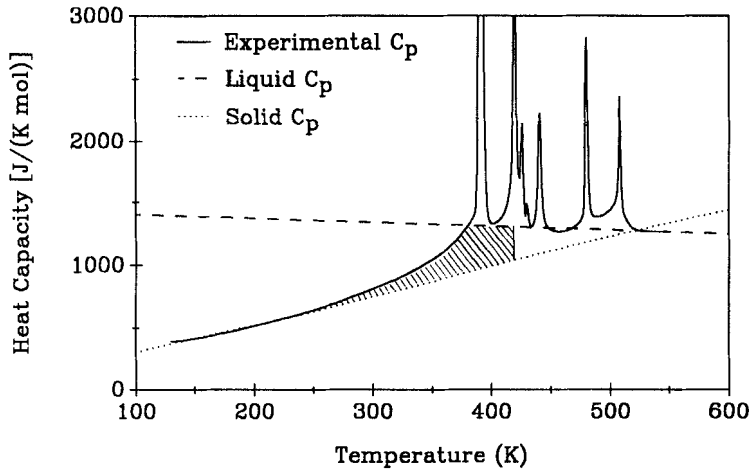

FIGURE 4 Comparison between the experimental C_p (solid line) and calculated C_p (dotted line) as well as liquid C_p (dashed line).

n-Octyloxy Groups. From previous work on *n*-paraffins it was shown that molecules such as octane start to show conformational disorder in the crystal from about 200 K.[6] At the melting temperature of octane (216 K), the heat capacity of the crystal is about 10% higher than expected from the vibration-only computation. Taking into account that the K3 to (K2 and K1) transition occurs in OOBPD more than 150 K higher in temperature and that the paraffinic chain is not as well ordered as in a paraffin crystal it is not surprising that the heat capacity is more than 40% higher and reaches the value of the liquid. One expects thus that the liquid heat capacity is linked to the large motion in the octyloxy groups.

As was pointed out in the discussion of the NMR data, the K3 and K1 transition changes approximately 5 *trans* bonds to the equilibrium *gauche* fraction in the liquid, so that K1 contains practically fully disordered flexible chains, not positionally and orientationally fixed mesogens.

The remaining high-temperature transitions between the various liquid crystalline phases were already described in the prior work.[2] Figure 5 shows that the baseline for all transitions is, however, practically the heat capacity of the liquid state and not a connection from the beginning to the end of each of the various endotherms. As a result, all transitions are somewhat larger than reported before. The total combined entropy is 106 J/(K mol) instead of 87.2 J/(K mol). The data of Table VI should thus replace the older data. It can also be seen from Table VI that crystal grown out of solution or melt showed only insignificant differences in thermal behaviors.

The transition temperatures listed in Table VI agree within one kelvin with the prior results. Either set is within typical DSC precision for transitions of such nature.

Finally, a speculation can be made about the ultimate low-temperature structure of OOBPD. There is no sharp glass transition, as one finds for the cooperative freezing of liquids to an amorphous glass, as well as no further first order transition. One expects thus that the attached paraffinic chains gain order continuously on cooling, without changing the *gauche*-to-*trans* ratio significantly (as shown by the

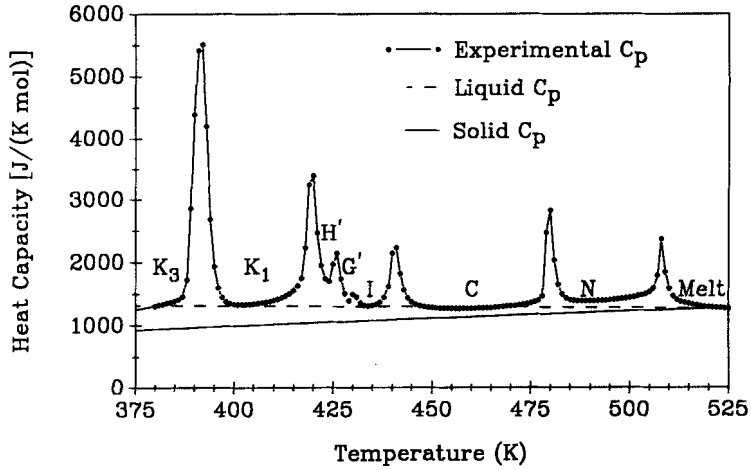

FIGURE 5 Section plot of Figure 4 from 375 to 525 K showing proper baseline offered by the liquid heat capacity (dashed line).

NMR evidence). This type of ordering must, since it occurs over such a broad temperature range, also be a rather local ordering to avoid cooperative freezing in form of a crystallization or glass formation. Comparing with our earlier estimate[2] that a molecule like OOBPD should have an overall entropy of fusion of about 210 J/(K mol) (152 J/(K mol) for the flexible chains, rest for the mesogen), one can see that at about 250 K the experimental data are within 30 J/(K mol) of this value (106 J/(K mol) from the transitions and 74.7 J/(K mol) for the increased heat capacity). The entropy of an amorphous, CH_2— group at absolute zero[36] derived from polyethylene heat capacity and heats of fusion is 3 J/(K mol), just the right amount for the 10 bonds marked with a ¤ in Figure 3 between Ar and C-14 to be in a state similar to glassy polyethylene.

CONCLUSIONS

A detailed account has been given for the order and motion in OOBPD. As suggested before, all liquid crystalline phases have full conformational disorder and motion. The K1 phase is still fully conformationally disordered (condis crystal), only the mesogen has gained orientational and positional order. Ring flipping by 180° is still possible in K1, but freezes at about 336 K in the K3 phase. The transition from K1 and K3 involves the fixing of 5–6 specific bonds in the two octyloxy chains predominately in the *trans* conformation. The remaining 10 bonds show a very high heat capacity in the K3 phase that ultimately drops at 200–250 K to the heat capacities of a vibrator with a residual entropy close to that expected for glassy polyethylene. Specific geometries and correlation times could be suggested and a link to the thermally induced defect motion in paraffins could be made.

Acknowledgment

This work was supported by the Division of Materials Research, National Science Foundation, Polymers Program, Grant #DMR 8818412 and the Division of Materials Sciences, Office of Basic Energy Sciences, U.S. Department of Energy, under Contract DE-AC05-84OR21400 with Martin Marietta Energy Systems, Inc.

References

1. B. Wunderlich, M. Möller and H. G. Wiedemann, *Mol. Cryst. Liq. Cryst.*, **140**, 211 (1986).
2. H. G. Wiedemann, J. Grebowicz and B. Wunderlich, *Mol. Cryst. Liq. Cryst.*, **140**, 219 (1986).
3. M. Cao, J. Wesson, K. Loufakis and B. Wunderlich, *Mol. Cryst. Liq. Cryst.*, **140**, 231 (1986).
4. M. Möller, D. Oelfin and B. Wunderlich, *Mol. Cryst. Liq. Cryst.*, **173**, 101 (1989).
5. B. Wunderlich and J. Grebowicz, *Adv. Polymer Sci.*, **60/61**, 1 (1984).
6. Y. Jin and B. Wunderlich, *J. Phys. Chem.*, to be published (1991).
7. G. W. Gray, J. B. Hartley, A. Ibbotson and B. Jones, *J. Chem. Soc.*, 4359 (1955).
8. F. D. Doty and P. D. Ellis, *Review of Scientific Instruments*, December (1981).
9. A. L. van Geat, *Abstracts of the 10th Experimental NMR Conferences,* Mellon Institute, Pittsburgh, PA, March, 1969.
10. Y. Jin and B. Wunderlich, *J. Thermal Analysis*, **36**, 765 (1990).
11. Y. Jin and B. Wunderlich, *J. Thermal Analysis*, **36**, 1519 (1990).
12. Y. Jin and B. Wunderlich, *J. Thermal Analysis*, to be published (1992).
13. R. Pan, M. Varma and B. Wunderlich, *J. Thermal Analysis*, **35**, 955 (1989).
14. R. M. Silverstein, G. C. Bassler and T. C. Morrill, "Spectrometric Identification of Organic Compounds," John Wiley & Sons, New York (1981).
15. Sadtler Research Lab., ^{13}C NMR Spectra Collection.
16. J. B. Stothers, "Carbon-13 NMR Spectroscopy," Academic Press, New York (1972).
17. A. N. Garroway, W. B. Moniz and H. A. Resing, *Prepr. Div. Org. Coatings Plastics Chem., Am. Chem. Soc.*, **36**, 133 (1976).
18. A. N. Garroway, W. B. Moniz and H. A. Resing, *ACS Symp. Ser., No. 103*, 67 (1979).
19. J. R. Lyerla, C. S. Yannoni and C. A. Fyfe, *Acc. Chem. Res.*, **15**, 208 (1982).
20. C. A. Fyfe, J. R. Lyerla, W. Volksen and C. S. Yannoni, *Macromolecules*, **12**, 757 (1979).
21. B. Wunderlich, "Macromolecular Physics, Vol. 3, Crystal Melting," Academic Press, New York (1980).
22. J. Sandström, "Dynamic NMR Spectroscopy," Chapter 6, Academic Press, New York (1982).
23. A. E. Tonelli and F. C. Schilling, *Acc. Chem. Res.*, **14**, 233 (1981).
24. F. A. Bovey, "Chain Structure and Conformation of Macromolecules," Academic Press, New York (1982).
25. A. E. Tonelli, "NMR Spectroscopy and Polymer Microstructure: The Conformational Connection," VCH Publishers, New York (1989).
26. P. J. Flory, "Statistical Mechanics of Chain Molecules," Wiley-Interscience, New York (1969).
27. See for example, A. E. Woodward, A. Odajima and J. A. Sauer, *J. Phys. Chem.*, **65**, 1384 (1961).
28. A. E. Tonelli, "Encyclopedia of Polymer Science and Engineering," sec. ed., Vol. 4, p. 120, Wiley, New York (1986).
29. W. Pechhold, *Kolloid Z. Z. Polymer*, **241**, 955 (1968).
30. B. Wunderlich, M. Möller, J. Grebowicz and H. Baur, *Adv. Polymer Sci.*, **87**, 1 (1988).
31. J. Schaefer, E. O. Stejskal and R. Buchdahl, *Macromolecules*, **10**, 384 (1977).
32. D. L. VanderHart, W. L. Earl and A. N. Garraway, *J. Magn. Reson.*, **44**, 361 (1981).
33. U. Haeberlin, *"High Resolution NMR in Solids," Adv. Magn. Reson.*, Supplement 1 (1976).
34. J. Cheng and B. Wunderlich, unpublished results.
35. B. Wunderlich and H. Bauer, *Adv. Polymer Sci.*, **7**, 151 (1970).
36. *ATHAS* data bank, University of Tennessee, Knoxville, TN 37996-1600 (1991).